

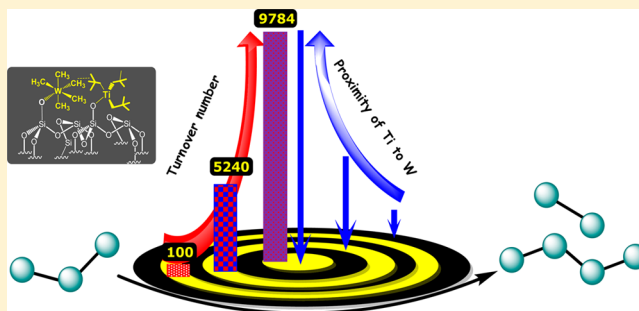
Unearthing a Well-Defined Highly Active Bimetallic W/Ti Precatalyst Anchored on a Single Silica Surface for Metathesis of Propane

Manoja K. Samantaray,* Santosh Kavitate, Natalia Morlanés, Edy Abou-Hamad, Ali Hamieh, Raju Dey, and Jean-Marie Basset*[✉]

King Abdullah University of Science and Technology, KAUST Catalysis Center (KCC), Thuwal 23955-6900, Saudi Arabia

Supporting Information

ABSTRACT: Two compatible organometallic complexes, $W(Me)_6$ (1) and $Ti(Np)_4$ (2), were successively anchored on a highly dehydroxylated single silica support (SiO_{2-700}) to synthesize the well-defined bimetallic precatalyst $[(\equiv Si-O-)W(Me)_5(\equiv Si-O-)Ti(Np)_3]$ (4). Precatalyst 4 was characterized at the molecular level using advanced surface organometallic chemistry (SOMC) characterization techniques. The strong autocorrelation observed between methyl of W and Ti in $^1H-^1H$ multiple-quantum NMR spectra demonstrates that W and Ti species are in close proximity to each other. The bimetallic precatalyst 4, with a turnover number (TON) of 9784, proved to be significantly more efficient than the silica-supported monometallic catalyst $[(\equiv Si-O-)W(Me)_5]$ (3), with a TON of 98, for propane metathesis at 150 °C in a flow reactor. The dramatic improvement in the activity signifies the cooperativity between Ti and W and indicates that the key step of alkane metathesis (C–H bond activation followed by β -H elimination) occurs on Ti, followed by olefin metathesis, which occurs on W. We have demonstrated the influence and importance of proximity of Ti to W for achieving such a significantly high activity. This is the first report demonstrating the considerably high activity (TON = 9784) in propane metathesis at moderate temperature (150 °C) using a well-defined bimetallic system prepared via the SOMC approach.



INTRODUCTION

Over the last 20 years, since the discovery of a silica-supported catalyst for the alkane metathesis reaction,¹ our group has been extensively working on the development of well-defined single-site supported catalytic systems for the alkane metathesis reaction,^{2–6} while Brookhart and co-workers^{7,8} and Burnett and Hughes⁹ aimed at tandem systems. There have been several reports of group 4 to group 6 oxide-supported catalysts, including by us, for various organic transformation reactions involving C–H and C–C bond activation,^{10–13} low-temperature hydrogenolysis of linear alkanes,¹⁴ olefin metathesis,^{15–17} and alkane metathesis,^{18–20} to name a few. During these developments, we observed primary products and demonstrated that alkane metathesis on Ta-based catalysts was a kind of “single-site cascade reaction” in which dehydrogenation of the alkane to give the olefin followed by olefin metathesis and hydrogenation of these olefins occurred on the same metal.²¹ We predicted that the reactivity of the catalyst could be improved if it were sufficiently electron-deficient to achieve C–H bond activation leading to dehydrogenation of alkanes to give olefins (with subsequent metathesis and hydrogenation of these olefins). To validate our working hypothesis, our first strategy was to support tantalum on a silica support on which we previously grafted a zirconium hydroxyl.¹² As expected, this catalyst showed improved activity in the propane metathesis reaction compared with silica-supported tantalum (the turnover

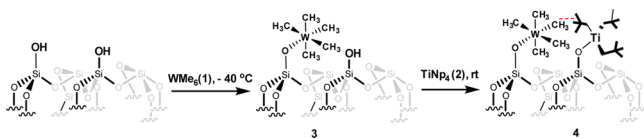
number (TON) increased from 60 to 100).¹² This better understanding of reaction mechanisms led us to the design of the best catalyst.^{22–25} With the concept of catalysis by design, we recently reported a well-defined silica-supported bimetallic system consisting of W and Zr.²⁶ By this move we could increase the TON from 150 to 1400 in the *n*-decane metathesis reaction. Our group has also discovered that oxide-supported Ti complexes are better catalysts than Zr complexes for low-temperature hydrogenolysis of paraffins.^{14,27} It should be noted that the first step of this reaction is a C–H bond dissociation. The cooperative effect observed in the case of the W/Zr bimetallic system and the higher reactivity of titanium hydrides compared with zirconium hydrides in low-temperature hydrogenolysis reactions tempted us to associate Ti with W and synthesize a well-defined W/Ti bimetallic system. We thus used the best metal for each of the required elementary steps: Ti for C–H activation followed by β -H elimination and W for olefin metathesis.

Herein we disclose a well-defined bimetallic system supported on a single (silica) surface for metathesis of propane, $[(\equiv Si-O-)W(Me)_5(\equiv Si-O-)Ti(Np)_3]$ (4) (Np = neopentyl) (Scheme 1). We characterized this bimetallic system at the molecular level using modern characterization techniques of

Received: December 17, 2016

Published: February 10, 2017

Scheme 1. Synthesis of Supported $[(\equiv\text{Si}-\text{O})\text{W}(\text{Me})_5(\equiv\text{Si}-\text{O})\text{Ti}(\text{Np})_3]$ (4**)**



surface organometallic chemistry (SOMC). This precatalyst **4** proved to be very efficient in propane metathesis, with a significantly higher TON of 9784 and an initial turnover frequency (TOF) of 900 h^{-1} , compared with the monometallic system $[(\equiv\text{Si}-\text{O})\text{W}(\text{Me})_5]$ (**3**), which provided a low TON of 98 with an initial TOF of 15 h^{-1} in the propane metathesis reaction under identical conditions. A similar approach was used by Brookhart and co-workers^{7,8} and previously by Burnett and Hughes,⁹ but our approach was to make the catalyst *single site by design* starting from mechanistic considerations, and we have reached the best TON ever observed in propane metathesis.

RESULTS AND DISCUSSION

Preparation and Characterization of $[(\equiv\text{Si}-\text{O})\text{W}(\text{Me})_5(\equiv\text{Si}-\text{O})\text{Ti}(\text{Np})_3]$ (4**) on SiO_{2-700} .** We previously reported the synthesis of silica-supported $[(\equiv\text{Si}-\text{O})\text{W}(\text{Me})_5]$ (**3**) and $[(\equiv\text{Si}-\text{O})\text{Ti}(\text{Np})_3]$ with molecular-level characterization using solid-state NMR, IR, elemental analysis, and gas quantification methods.^{23,28} This is the first report demonstrating the successive anchoring of the homogeneous organometallic complexes $\text{W}(\text{Me})_6$ (**1**) at -40 °C and TiNp_4 (**2**) at 25 °C on a single silica surface (SiO_{2-700} , which contain 0.23–0.26 mmol of silanol groups per gram) under an inert atmosphere of argon (Scheme 1).

Elemental analysis of **4** showed it to have the composition 0.39 wt % W, 1.10 wt % Ti, and 4.12 wt % C (the expected C content should be 4.24 wt % for both metal atoms).

The IR spectrum of **4** (Figure 1) shows the complete disappearance of the bands at 3744 cm^{-1} , which are associated with isolated and geminal silanols. For **4**, two new groups of bands are observed in the region of $3021\text{--}2787\text{ cm}^{-1}$ and at 1465 and 1365 cm^{-1} . These are assigned to $\nu(\text{CH})$ and $\delta(\text{CH})$ vibrations of the methyl and neopentyl ligands bonded to tungsten and titanium, respectively.

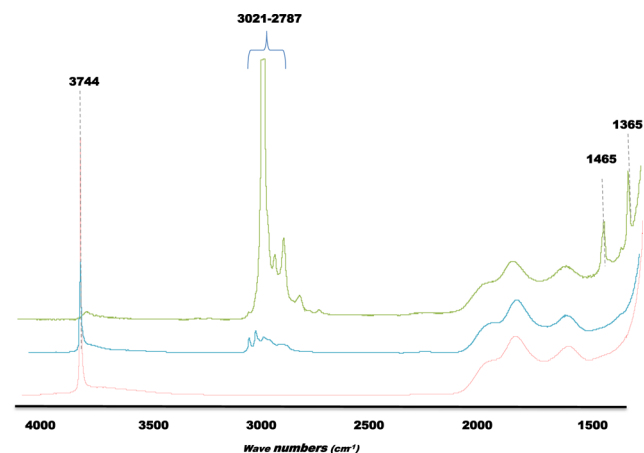


Figure 1. IR spectra of SiO_{2-700} (red), $[(\equiv\text{Si}-\text{O})\text{W}(\text{Me})_5]$ (**3**) (blue), and $[(\equiv\text{Si}-\text{O})\text{W}(\text{Me})_5(\equiv\text{Si}-\text{O})\text{Ti}(\text{Np})_3]$ (**4**) (green).

Further characterization of **4** was done using solid-state NMR spectroscopy. The ^1H magic-angle spinning (MAS) solid-state NMR spectrum of **4** (Figure 2A) displays two signals

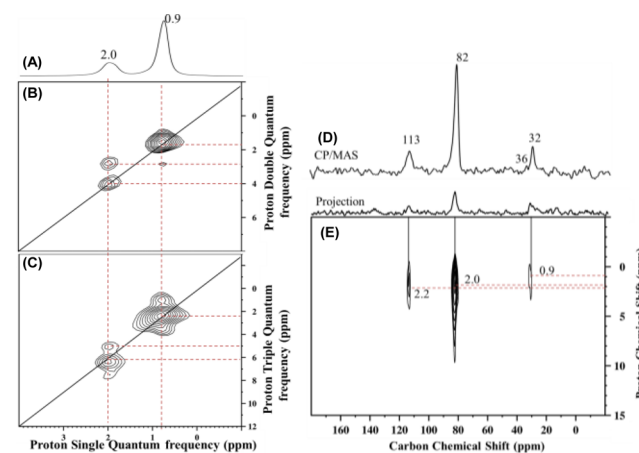


Figure 2. (A) One-dimensional (1D) ^1H MAS solid-state NMR spectrum of **4** acquired at 600 MHz (14.1 T) with a MAS frequency of 22 kHz, a repetition delay of 5 s, and eight scans. (B) Two-dimensional (2D) ^1H – ^1H double-quantum (DQ)/single-quantum (SQ) and (C) ^1H – ^1H triple-quantum (TQ)/SQ NMR spectra of **4** (both acquired with 32 scans per t_1 increment, a repetition delay of 5 s, and 128 individual t_1 increments). (D) ^{13}C CP/MAS NMR spectrum of **4** (acquired at 9.4 T ($\nu_0(^1\text{H}) = 400$ MHz) with a MAS frequency of 10 kHz, 10 000 scans, a repetition delay of 4 s, and a contact time of 2 ms). Exponential line broadening of 80 Hz was applied prior to Fourier transformation. (E) 2D ^1H – ^{13}C CP/MAS dipolar HETCOR spectrum of **4** (acquired at 9.4 T with a MAS frequency of 10 kHz, 3000 scans per t_1 increment, a repetition delay of 4 s, 64 individual t_1 increments, and a contact time of 0.2 ms). For all of the spectra depicted here, only W–Me in **4** was 70% ^{13}C -labeled.

at 2.0 and 0.9 ppm, and it should be noted that the methylene of Ti come along with methyl of W. Strong autocorrelation peaks were observed for 0.9 and 2.0 ppm in double-quantum (DQ) (1.8 and 4.0 in the indirect dimensions) and triple-quantum (TQ) (2.7 and 6.0 ppm in the indirect dimensions) NMR experiments under 22 kHz MAS, as shown in Figure 2B,C, respectively. These strong autocorrelation peaks were attributed to the methyl groups of W and Ti. Interestingly, we also observed a correlation outside the diagonal between the methyls of W (2.0 ppm) and methyls of Ti–Np (0.9 ppm), confirming that these two groups are unexpectedly in proximity to each other in space (Figure 2).

The ^{13}C cross-polarization MAS (CP/MAS) NMR spectrum of an enriched sample of **4** (in which only tungsten methyls were 70% ^{13}C -enriched) shows four peaks, at 82 ppm for W– CH_3 , 113 ppm for Ti– CH_2 , 36 ppm for Ti– $\text{CH}_2\text{--C}(\text{CH}_3)_3$, and 32 ppm for Ti– $\text{CH}_2\text{--C}(\text{CH}_3)_3$ (Figure 2D), which are correlated with the proton resonances at 2.0 ppm for W– CH_3 , 2.2 ppm for Ti– CH_2 , and 0.9 ppm for Ti– $\text{CH}_2\text{--C}(\text{CH}_3)_3$, respectively, as indicated in the 2D ^1H – ^{13}C heteronuclear correlation (HETCOR) NMR spectrum recorded with a contact time of 0.2 ms (Figure 2E).

The ^1H and ^{13}C chemical shifts are similar to those observed in the solution NMR spectra of molecular species of **1** and **2** (Figures S1–S5). It should be noted that during the synthesis of **4** there is the possibility of forming monopodal or bipodal grafted species because of strained silica ring defects produced after thermal dehydroxylation. However, the absence of a signal

Table 1. Propane Metathesis Reaction: Activities (TONs) and Alkane Product Selectivities of 4 and Other W Catalyst Precursors at 150 °C

catalyst precursor	TON (conv.) ^a	product selectivity (%) ^b				
		methane	ethane	butanes ^c	pentanes ^d	ref
[≡SiO ₂₋₇₀₀ -W(Me) ₅]	127 (12%)	2	54	33/4	6/1	16
[≡SiO ₂₋₂₀₀ -W(Me) ₅]	47 (5%)	7	56	22/2.5	9/2	16
[≡SiO ₂₋₇₀₀ -W=CH ₂ (H) _x]	261 (29%)	3	58	27/5	4.5/2	18
[(≡Si-O-)W(H) _x]	154 (17%)	5.7	56	29/2.8	5.1/1.4	18
4 ^e	1772 (17%)	4	52	38/2	4/1	this work

^aTON is expressed in moles of propane transformed per mole of W. ^bProduct selectivity is defined as 100% times the amount of product divided by the total amount of products. For butanes and propanes, linear/branched ratios are shown. ^cC₄/i-C₄. ^dC₅/i-C₅. ^ePrecursor [(≡Si-O-)W(Me)₅(≡Si-O-)Ti(Np)₃] (4) with a W loading of 0.34 wt % and a Ti loading of 1.02 wt % with a Ti/W ratio of 11.5 was used to carry out the catalytic reaction.

at or near 0.0 ppm in the ¹H and ¹³C solid-state NMR spectra excludes the formation of bipodal species [(≡Si-O)_{1+n}W(Me)_{5-n}(≡Si-O)_{1+m}Ti(Np)_{3-m}](≡Si-R) (R = Me, n = 1, m = 0 or R = Np, n = 0, m = 1) via transfer of methyl or neopentyl to an adjacent silicon atom of silica. The supported complex was thermally treated at 80 °C to observe the carbyne species, which were already observed in our previous studies (Figures S6 and S7).^{23,26}

Evaluation of the Catalytic Activity of 4 and Comparison with Existing Catalysts for the Propane Metathesis Reaction.

We developed a concept of anchoring two metals on a single surface in order to have them in proximity to each other, believing that one could carry out dehydrogenation and then the other could perform metathesis, so that we could increase the rate as well as TON in the alkane metathesis reaction. After the successful synthesis and characterization of complex 4, we investigated its efficiency as a catalyst precursor for the propane metathesis reaction. To evaluate the catalytic activity of newly designed catalyst 4 and compare it with those of other existing catalysts, we maintained identical reaction conditions (batch reactor with propane at 0.9 atm at 150 °C for 3 days) with a W loading of 0.34 wt % and a Ti loading of 1.02 wt % for species 4. The experimental results confirm our hypothesis, with very high TON (1772) compared with the existing catalysts [(≡Si-O-)W(≡C^tBu)(CH₂^tBu)₂] (TON = 0),²⁰ [(≡Si-O-)W(Me)₅] (TON = 127), [(≡Si-O-)W(H)_x] (TON = 154), and [(≡Si-O-)W=CH₂(H)_x] (TON = 261). Propane was successfully converted to methane, ethane, butanes, and pentanes (Table 1).

The greater TON using precatalyst 4 (Table 1) clearly demonstrates the influence of Ti in close proximity to W. Strategically to further investigate the influence and importance of Ti in proximity to W, we decided to study this reaction under continuous-flow reaction conditions, where our catalyst would be exposed to fresh reactant continuously. Another advantage of the continuous-flow reaction was that we could also study the propane metathesis reaction using separately prepared silica-supported [(≡Si-O-)W(Me)₅] (3) and [(≡Si-O-)Ti(Np)₃], i.e., we could have different layers of these catalysts, which could provide an understanding of the influence of the close proximity of the metal centers in the bimetallic system.

The metathesis of propane was carried out in a continuous-flow reactor using catalyst precursor 4. The reaction continued for 50 h at 150 °C in a flow of propane (5 mL/min propane, weight hourly space velocity (WHSV) = 5.4 h⁻¹, volume hourly space velocity (VHSV) = 2700 h⁻¹), and the highest TON was 9784 (Figure 3). Continuing the reaction for a further 24 h

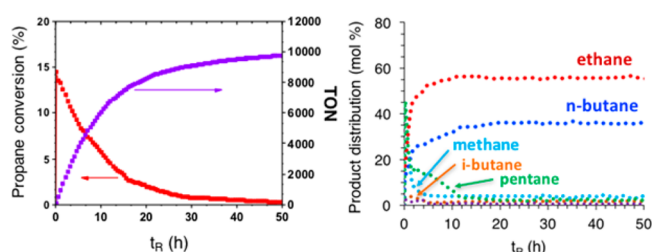


Figure 3. Turnover number (TON) and product distribution obtained during the metathesis of propane catalyzed by [(≡Si-O-)W(Me)₅(≡Si-O-)Ti(Np)₃] (4) (0.34 wt % W and 1.02 wt % Ti) in a continuous-flow reactor.

resulted in an additional increase in conversion as well as in TON to 10100, which is the highest TON ever observed in the propane metathesis reaction.

The higher TON in the flow reactor compared with the batch reactor is understandable because the catalyst is always exposed to fresh reactant instead of reactant and products (generated from the reactant). In contrast, in the case of a batch reactor not only the reactant but also the products can interact with the catalyst, hence increasing the risk of competition between the reactant and the resulting products.

Additionally, to prove that there is a cooperative effect between the two metals on the same surface, we carried out the reaction under layer conditions, keeping the reactant to catalyst ratio intact. As explained in Figure 4, we tried three types of catalytic beds: the first was just the supported bimetallic system, the second was a succession of a first layer of [(≡Si-O-)Ti(Np)₃] followed by a layer of [(≡Si-O-)W(Me)₅] separated by glass wool (denoted as Ti/W), and the third was a bed constituted of a mechanical mixture of [(≡Si-O-)Ti(Np)₃] and [(≡Si-O-)W(Me)₅] (denoted as Ti+W), keeping the weight percentages of the metals identical in every case. The results obtained from these different types of layer conditions prove that the TON of the propane metathesis reaction with both metals present separately (TON_{Ti/W} = 689; TON_{Ti+W} = 5240) is considerably higher than those for the corresponding monometallic systems (TON_W = 98; TON_{Ti} = 43) but lower than that with bimetallic precatalyst 4 (TON = 9784) (Figure 4). We also carried out another layered experiment with the succession of a first layer of [(≡Si-O-)W(Me)₅] followed by a layer of [(≡Si-O-)Ti(Np)₃] separated by glass wool, which gave a TON of 639. These results clearly prove the importance of having Ti in proximity to W for achieving such a high activity in terms of TON (Figure 4).

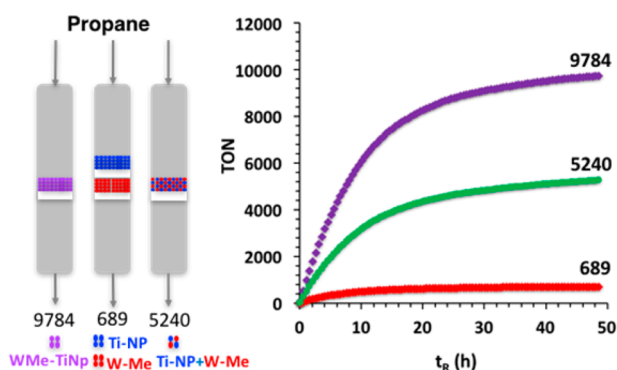


Figure 4. Turnover number vs time for precatalyst $[(\equiv\text{Si}-\text{O}-)\text{W}(\text{Me})_5(\equiv\text{Si}-\text{O}-)\text{Ti}(\text{Np})_3]$ (**4**) (0.34 wt % W and 1.02 wt % Ti) (violet color), the mixture of $[(\equiv\text{Si}-\text{O}-)\text{W}(\text{Me})_5]$ and $[(\equiv\text{Si}-\text{O}-)\text{Ti}(\text{Np})_3]$ (0.27 wt % W, 1.05 wt % Ti) (green color), and a layer of $[(\equiv\text{Si}-\text{O}-)\text{Ti}(\text{Np})_3]$ (1.1 wt % Ti) followed by a layer of $[(\equiv\text{Si}-\text{O}-)\text{W}(\text{Me})_5]$ (0.34 wt % W) (red color). TON is expressed in moles of propane transformed per mole of W.

Furthermore, we took advantage of the flow reactor to try to understand the formation of the primary products by studying the effect of the contact time (proportional to the inverse of the space velocity) on the propane conversion and product selectivity (Figure 5). First, using a constant flow of propane

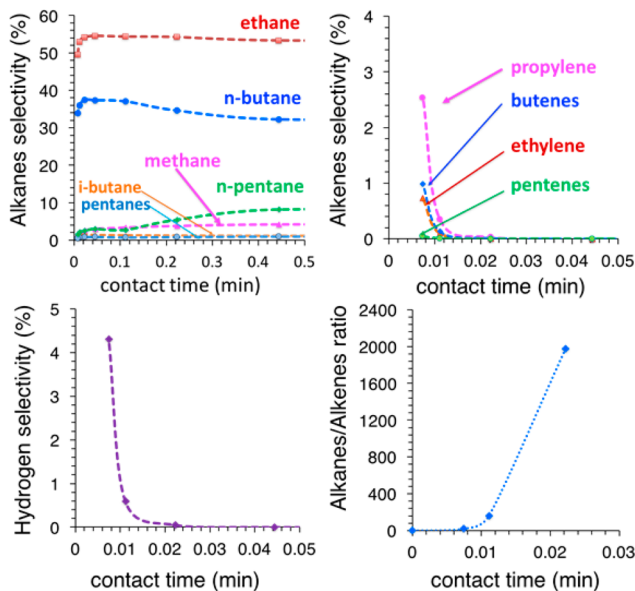


Figure 5. Metathesis of propane in a continuous-flow reactor (150 °C, 1 atm, 100 mg of $[(\equiv\text{Si}-\text{O}-)\text{W}(\text{Me})_5(\equiv\text{Si}-\text{O}-)\text{Ti}(\text{Np})_3]$ (**4**) (0.34 wt % W and 1.02 wt % Ti). Selectivity vs contact time for alkanes, alkenes, and H_2 and alkanes/alkenes ratio vs contact time are shown.

(5 mL min⁻¹, contact time = 0.022 min) at 150 °C, we initially observed the formation of methane, ethane, butane, pentane, and hydrogen from C–H bond activation of propane followed by metathesis, in agreement with previous studies.²¹ After 10 h, nearly constant selectivities were observed for propane metathesis as follows: 4% methane, 56% ethane, 2.5% isobutane, 35% butane, 0.5% isopentane, and 2% pentane. The linear products were always favored over the branched ones, in agreement with the values observed under batch conditions (Table 1 and Figures 3 and 5).

Second, when the propane flow rate was varied over a wide range between 0.1 and 15 mL min⁻¹ (VHSV = 43–8100 h⁻¹), the conversion increased linearly with contact time (Figure S8), which indicates that the rate was not diffusion-limited. The extrapolated selectivity at zero contact time provides information on the primary products (Figures 5 and S8). With decreasing contact time, a strong increase in the proportion of H_2 and alkenes (from C_2 to C_4) and a parallel decrease in the production of alkanes are observed, decreasing the alkanes/alkenes ratio until it reaches 0 at extrapolated zero contact time (Figures 5 and S8). These data indicate that olefins and H_2 are the primary products, in agreement with previously reported kinetic studies.²¹

CONCLUSION

Two chemically compatible organometallic complexes were anchored on a single surface (SiO_{2-700}) without interfering with each other. The surface complex was characterized at the molecular level by advanced solid-state NMR, IR, elemental analysis, and gas quantification methods. It was observed that titanium and tungsten species are very close to each other in space (strong autocorrelation of the methyls in $^1\text{H}-^1\text{H}$ double-quantum spectra).

Anchoring the two single sites in proximity to each other on a single surface is obviously more efficient (TON ca. 10000) than mechanical mixing of the two catalysts (TON ca. 5500) or using separate-layer beds (TON ca. 700). This cooperative effect of two different metals anchored on the same surface influencing the reactivity in a given reaction (e.g., alkane metathesis) opens up new perspectives for the synthesis of various supported bimetallic systems via the SOMC approach and many cascade reactions in “single-site systems”.

EXPERIMENTAL SECTION

General Procedures. All experiments were carried out using standard Schlenk and glovebox techniques under an inert argon atmosphere. The syntheses and treatments of the surface species were carried out using high-vacuum lines (<10⁻⁵ mbar) and glovebox techniques. Pentane was distilled from a Na/K alloy under argon and dichloromethane from CaH_2 . Both solvents were degassed through freeze–pump–thaw cycles. SiO_{2-700} was prepared from Aerosil silica from Degussa (specific area of 200 m²/g), which was partly dehydroxylated at 700 °C under high vacuum (<10⁻⁵ mbar) for 24 h to give a white solid having a specific surface area of 190 m²/g and containing 0.5–0.7 OH/nm². Propane was dried and deoxygenated before use by passage through a mixture of freshly regenerated molecular sieves (3 Å) and R3-15 catalyst (BASF). IR spectra were recorded on a Nicolet 6700 FT-IR spectrometer by using a diffuse-reflectance infrared Fourier transform (DRIFT) cell equipped with CaF_2 windows. The IR samples were prepared under argon within a glovebox. Typically, 64 scans were accumulated for each spectrum (resolution = 4 cm⁻¹). Elemental analyses were performed at Mikroanalytisches Labor Pascher (Germany) and ACL KAUST. Gas-phase analysis of alkanes was performed using an Agilent 6850 gas chromatography column with a split injector coupled with a flame ionization detector. An HP-PLOT Al_2O_3 KCl capillary column (30 m × 0.53 mm; 20.00 mm) coated with a stationary phase of aluminum oxide deactivated with KCl was used with helium as the carrier gas at 32.1 kPa. Each analysis was carried out under the same conditions: a flow rate of 1.5 mL/min and an isotherm at 80 °C. Organometallic complexes **1** and **2** and their corresponding silica-supported complexes were prepared according to literature procedures.^{28–30}

Liquid-State NMR Spectroscopy. All of the liquid-state NMR spectra were recorded on Bruker Avance 600 MHz spectrometers. All of the chemical shifts were measured relative to the residual ^1H or ^{13}C resonance in the deuterated solvent (CD_2Cl_2 or C_6D_6).

Solid-State NMR Spectroscopy. One-dimensional ^1H MAS and ^{13}C CP/MAS solid-state NMR spectra were recorded on Bruker AVANCE III spectrometers operating at 400 or 600 MHz resonance frequencies for ^1H . The 400 MHz experiments employed a conventional double-resonance 4 mm CP/MAS probe, while experiments at 600 MHz utilized a 3.2 mm HCN triple-resonance probe. In all cases, the samples were packed into rotors under an inert atmosphere inside gloveboxes. Dry nitrogen gas was utilized for sample spinning to prevent degradation of the samples. NMR chemical shifts are reported with respect to the external references tetramethylsilane and adamantane. For ^{13}C CP/MAS NMR experiments, the following sequence was used: a 90° pulse on the proton (pulse length = 2.4 s), then a cross-polarization step with a contact time of typically 2 ms, and finally acquisition of the ^{13}C signal under high-power proton decoupling. The delay between the scans was set to 4 s to allow the complete relaxation of the ^1H nuclei, and the number of scans ranged between 10 000 and 20 000 for ^{13}C and was eight for ^1H . An exponential apodization function corresponding to a line broadening of 80 Hz was applied prior to Fourier transformation.

The 2D ^1H – ^{13}C HETCOR solid-state NMR spectroscopy experiments were conducted on a Bruker AVANCE III spectrometer operating at 400 MHz using a 3.2 mm MAS probe. The experiments were performed according to the following scheme: 90° proton pulse, t_1 evolution period, CP to ^{13}C , and detection of the ^{13}C magnetization under two-pulse phase-modulated decoupling. For the cross-polarization step, a ramped radiofrequency (RF) field centered at 75 kHz was applied to the protons, while the ^{13}C channel RF field was matched to obtain optimal signal. A total of 32 or 64 t_1 increments with 3000 scans each were collected. The sample spinning frequency was 10 kHz. With a short contact time (0.2 ms) for the CP step, the polarization transfer in the dipolar correlation experiment was verified to be selective for the first coordination sphere about the tungsten, i.e., to lead to correlations only between pairs of attached ^1H – ^{13}C spins (C–H directly bonded).

^1H – ^1H Multiple-Quantum Spectroscopy. Two-dimensional double-quantum (DQ) and triple-quantum (TQ) experiments were recorded on a Bruker AVANCE III spectrometer operating at 600 MHz with a conventional double-resonance 3.2 mm CP/MAS probe according to the following general scheme: excitation of DQ coherences, t_1 evolution, z filter, and detection. The spectra were recorded in a rotor-synchronized fashion in t_1 by setting the t_1 increment equal to one rotor period. One cycle of the standard back-to-back (BABA) recoupling sequences was used for the excitation and reconversion period.³¹ Quadrature detection in w_1 was achieved using the States-TPPI method. A MAS frequency of 20 kHz was used. The 90° proton pulse length was 2.5 μs , and a recycle delay of 5 s was used. A total of 128 t_1 increments with 32 or 128 scans per increment were recorded. The DQ frequency in the w_1 dimension corresponds to the sum of two single-quantum (SQ) frequencies of two coupled protons and is correlated in the w_2 dimension with the two corresponding proton resonances.³² The TQ frequency in the w_1 dimension corresponds to the sum of three SQ frequencies of three coupled protons and is correlated in the w_2 dimension with the three individual proton resonances. Conversely, groups of less than three equivalent spins will not give rise to diagonal signals in this spectrum.

Preparation of Supported Complex 4 on SiO_2 –700. A solution of **1** in pentane (30 mg, 0.11 mmol) was reacted with 2.0 g of Aerosil SiO_2 –700 at -40°C for 3 h, and the product was filtered, washed with pentane (3×20 mL), and dried for 20 min under vacuum (see Figure S9 for the NMR analysis). The resulting light-yellow powder was transferred to another double Schlenk tube, to which a pentane solution of excess **2** (201 mg, 0.6 mmol) was added at room temperature, and the reaction was continued at that temperature for another 3 h. At the end of the reaction, the resulting light-yellow solid was washed with pentane (3×20 mL) and dried under dynamic vacuum ($<10^{-5}$ Torr) for 1 h. IR (cm^{-1}): 3021–2787, 1465, 1365. ^1H solid-state NMR (400 MHz): δ (ppm) = 2.0 (W– CH_3 and Ti– CH_2), 0.9 (– $\text{CH}_2(\text{CH}_3)_3$). ^{13}C CP/MAS solid-state NMR (100 MHz): δ (ppm) = 113.0 (Ti– CH_2), 82.0 (W– CH_3), 36.0 (Ti– CH_2 – $\text{C}(\text{CH}_3)_3$), 32.0 (Ti– CH_2 – $\text{C}(\text{CH}_3)_3$). Elemental analysis: 0.39 wt %

W, corresponding to $\sim 8\%$ of the silanols; 1.10 wt % Ti, corresponding to $\sim 89\%$ of the silanols (please note that the silanol density of SiO_2 –700 varies from 0.23 to 0.26 mmol/g); 4.12 wt % C (the expected C content should be 4.24 wt % for both metal atoms).

Typical Procedure for Propane Metathesis Reactions. A mixture of a potential catalytic material (0.0009 mmol of W and 0.011 mmol of Ti) and dry propane (853–890 hPa) was heated to 150°C in a batch reactor of known volume (280 mL) over a 3 day period. At the end of the run, an aliquot was drawn and analyzed by GC. The selectivity is defined as the amount of a particular product molecule divided by the total amount of products.

■ ASSOCIATED CONTENT

📄 Supporting Information

The Supporting Information is available free of charge on the ACS Publications website at DOI: 10.1021/jacs.6b12970.

Solution NMR spectra of **1** and **2**, thermal decomposition NMR spectra of **4**, and conversion versus time plot at high flow rate (PDF)

■ AUTHOR INFORMATION

Corresponding Authors

*jeanmarie.basset@kaust.edu.sa

*manoja.samantaray@kaust.edu.sa

ORCID

Jean-Marie Basset: 0000-0003-3166-8882

Notes

The authors declare no competing financial interest.

■ ACKNOWLEDGMENTS

The authors acknowledge the KAUST Nuclear Magnetic Resonance Core Lab and Analytical Core Lab (ACL) for the analysis of the sample. This publication is based upon work supported by the King Abdullah University of Science and Technology (KAUST) Office of Sponsored Research (OSR).

■ REFERENCES

- (1) Vidal, V.; Theolier, A.; Thivolle-Cazat, J.; Basset, J.-M. *Science* **1997**, 276 (5309), 99.
- (2) Taoufik, M.; Schwab, E.; Schultz, M.; Vanoppen, D.; Walter, M.; Thivolle-Cazat, J.; Basset, J. M. *Chem. Commun.* **2004**, 1434.
- (3) Soulivong, D.; Coperet, C.; Thivolle-Cazat, J.; Basset, J. M.; Maunders, B. M.; Pardy, R. B. A.; Sunley, G. J. *Angew. Chem., Int. Ed.* **2004**, 43, 5366.
- (4) Pelletier, J. D. A.; Basset, J. M. *Acc. Chem. Res.* **2016**, 49 (4), 664.
- (5) Samantaray, M. K.; Dey, R.; Abou-Hamad, E.; Hamieh, A.; Basset, J. M. *Chem. - Eur. J.* **2015**, 21, 6100.
- (6) Coperet, C.; Chabanas, M.; Saint-Arroman, R. P.; Basset, J. M. *Angew. Chem., Int. Ed.* **2003**, 42, 156.
- (7) Goldman, A. S.; Roy, A. H.; Huang, Z.; Ahuja, R.; Schinski, W.; Brookhart, M. *Science* **2006**, 312, 257.
- (8) Haibach, M. C.; Kundu, S.; Brookhart, M.; Goldman, A. S. *Acc. Chem. Res.* **2012**, 45 (6), 947.
- (9) Burnett, R. L.; Hughes, T. R. *J. Catal.* **1973**, 31, 55.
- (10) Thieuleux, C.; Maraval, A.; Veyre, L.; Coperet, C.; Soulivong, D.; Basset, J. M.; Sunley, G. J. *Angew. Chem., Int. Ed.* **2007**, 46, 2288.
- (11) Soignier, S.; Taoufik, M.; Le Roux, E.; Saggio, G.; Dablemont, C.; Baudouin, A.; Lefebvre, F.; de Mallmann, A.; Thivolle-Cazat, J.; Basset, J. M.; Sunley, G.; Maunders, B. M. *Organometallics* **2006**, 25, 1569.
- (12) Rataboul, F.; Coperet, C.; Lefort, L.; de Mallmann, A.; Thivolle-Cazat, J.; Basset, J. M. *Dalton Trans.* **2007**, 923.
- (13) Labinger, J. A.; Bercaw, J. E. *Nature* **2002**, 417, 507.

(14) Larabi, C.; Merle, N.; Norsic, S.; Taoufik, M.; Baudouin, A.; Lucas, C.; Thivolle-Cazat, J.; de Mallmann, A.; Basset, J. M. *Organometallics* **2009**, *28*, 5647.

(15) Taoufik, M.; Le Roux, E.; Thivolle-Cazat, J.; Basset, J. M. *Angew. Chem. Int. Ed.* **2007**, *46*, 7202.

(16) Rhers, B.; Salameh, A.; Baudouin, A.; Quadrelli, E. A.; Taoufik, M.; Coperet, C.; Lefebvre, F.; Basset, J. M.; Solans-Monfort, X.; Eisenstein, O.; Lukens, W. W.; Lopez, L. P. H.; Sinha, A.; Schrock, R. R. *Organometallics* **2006**, *25*, 3554.

(17) Leitch, D. C.; Lam, Y. C.; Labinger, J. A.; Bercaw, J. E. *J. Am. Chem. Soc.* **2013**, *135*, 10302.

(18) Thivolle-Cazat, J.; Coperet, C.; Soignier, S.; Taoufik, M.; Basset, J. M. *Nato. Sci. Ser. II. Math.* **2005**, *191*, 107.

(19) Taoufik, M.; Le Roux, E.; Thivolle-Cazat, J.; Coperet, C.; Basset, J. M.; Maunders, B.; Sunley, G. J. *Top. Catal.* **2006**, *40*, 65.

(20) Le Roux, E.; Taoufik, M.; Baudouin, A.; Coperet, C.; Thivolle-Cazat, J.; Basset, J. M.; Maunders, B. M.; Sunley, G. J. *Adv. Synth. Catal.* **2007**, *349*, 231.

(21) Basset, J. M.; Coperet, C.; Lefort, L.; Maunders, B. M.; Maury, O.; Le Roux, E.; Saggio, G.; Soignier, S.; Soulivong, D.; Sunley, G. J.; Taoufik, M.; Thivolle-Cazat, J. *J. Am. Chem. Soc.* **2005**, *127*, 8604.

(22) Le Roux, E.; Taoufik, M.; Coperet, C.; de Mallmann, A.; Thivolle-Cazat, J.; Basset, J. M.; Maunders, B. M.; Sunley, G. J. *Angew. Chem. Int. Ed.* **2005**, *44*, 6755.

(23) Samantaray, M. K.; Callens, E.; Abou-Hamad, E.; Rossini, A. J.; Widdifield, C. M.; Dey, R.; Emsley, L.; Basset, J. M. *J. Am. Chem. Soc.* **2014**, *136*, 1054.

(24) Chen, Y.; Abou-hamad, E.; Hamieh, A.; Hamzaoui, B.; Emsley, L.; Basset, J. M. *J. Am. Chem. Soc.* **2015**, *137*, 588.

(25) Maity, N.; Barman, S.; Callens, E.; Samantaray, M. K.; Abou-Hamad, E.; Minenkov, Y.; D'Elia, V.; Hoffman, A. S.; Widdifield, C. M.; Cavallo, L.; Gates, B. C.; Basset, J. M. *Chem. Sci.* **2016**, *7*, 1558.

(26) Samantaray, M. K.; Dey, R.; Kavitate, S.; Abou-Hamad, E.; Bendjeriou-Sedjerari, A.; Hamieh, A.; Basset, J. M. *J. Am. Chem. Soc.* **2016**, *138*, 8595.

(27) Rosier, C.; Niccolai, G. P.; Basset, J. M. *J. Am. Chem. Soc.* **1997**, *119*, 12408.

(28) Saint-Arroman, R. P.; Basset, J.-M.; Lefebvre, F.; Didillon, B. *Appl. Catal. A* **2005**, *290*, 181.

(29) Pfennig, V.; Seppelt, K. *Science* **1996**, *271*, 626.

(30) Shortland, A.; Wilkinson, G. *J. Chem. Soc., Chem. Commun.* **1972**, 318a.

(31) Sommer, W.; Gottwald, J.; Demco, D. E.; Spiess, H. W. *J. Magn. Reson., Ser. A* **1995**, *113*, 131.

(32) Rataboul, F.; Baudouin, A.; Thieuleux, C.; Veyre, L.; Coperet, C.; Thivolle-Cazat, J.; Basset, J. M.; Lesage, A.; Emsley, L. *J. Am. Chem. Soc.* **2004**, *126*, 12541.